Wavelet transform analysis directly from sinusoid crossings

Caesar Saloma*
National Institute of Physics, University of the Philippines, Diliman, Quezon City 1101, The Philippines
(Received 25 January 1995; revised manuscript received 2 May 1995)

We show that the wavelet transforms of an analog signal $f_a(t)$ can be computed directly and efficiently from a data representation consisting only of locations $\{t_i\}$, where $f_a(t)$ intersects with the reference sinusoid $r(t)$ of frequency W and amplitude A. To achieve a measurement bandwidth of W, one crossing must occur within each interval $\Delta=1/2W$. This is satisfied when $A \geq |f_a(t)|$ for all $f_a(t)$ values within the sampling period T. A total of $2M$ sinusoid crossings occur within T. Crossing-based wavelet analysis is demonstrated with respect to the sombrero-shaped wavelet, using 256 crossings of an interferogram signal.

PACS number(s): 02.70.−c, 89.80.+h, 02.60.Gf, 07.05.−t

Because of their good localization properties in both time and frequency domains, wavelet transforms (WT's) are well suited for multiresolution signal analysis [1,2]. Extraction of specific signal features using the WT technique has gained widespread interest in optics [3], audio [4], geophysics, solid state physics, astrophysics, weather forecasting, and medicine [5]. So far, WT analysis has been implemented only on data sets consisting of equally sampled values of the analog signal $f_a(t)$ where t is the independent (time) variable.

In this paper we show that WT's can be calculated directly and efficiently from a data set consisting only of locations of $\{t_i\}$ where $f_a(t)$ intersects with the reference sinusoid $r(t)$ of frequency W and amplitude A. Any sinusoid $r(t)=A\cos[2\pi(Wt+\phi)]$ can be utilized as reference signal, but choosing $\phi=0$ further simplifies the design of the crossing detector [6].

Because sinusoid crossing (SC) sampling is based on thresholding, it offers a simpler mode of signal acquisition than the amplitude sampling of $f_a(t)$. A SC detector can be built using only one comparator whose inputs are $r(t)$ and $f_a(t)$ [6]. A SC is detected every time the comparator output changes state as a result of sign flipping in the value of the input differential $[f_a(t)-r(t)]$. The largest measurable $f_a(t)$ value is limited only by the voltage compliance of the comparator.

As required by the Nyquist sampling criterion, a SC must occur within each interval Δ for the bandwidth of the sampled version $f(t)$ of $f_a(t)$, to be $2W=1/\Delta=2M/T$. This condition is satisfied when A is chosen such that $A \geq |f_a(t)|$ for all possible $f_a(t)$ values within T. The locations $\{t_i\}$ of the $2M$ SC's within T are indexed according to their order of detection in time ($i=1,2,\ldots,2M$).

The dynamic range of detection is optimized when A is made equal to the largest absolute $f_a(t)$ value $|f_a^{\max}|$. Because a SC cannot occur within a Δ wherein $|f_a(t)|>A$, $f(t)$ will be unknown within this interval. On the other hand, if $A \gg |f_a(t)|$ then small amplitude changes in $f_a(t)$ become difficult to observe. High-resolution (large M) signal analysis and synthesis have already been demonstrated in Fourier [7,8] and Hartley transform operations [9].

Investigations regarding the use of SC's as data representations have brought new insights into the roles of functional analysis and computational complexity in measurement processes [10]. This paper together with our previous work [7–9] illustrates that complicated signal processing operations can be done directly and efficiently from $\{t_i\}$. This is an important finding because many physical systems respond to external stimuli by thresholding. Note further that SC sampling can be formulated within the framework of the stochastic resonance technique [11]. For instance, it will be interesting to study whether the addition of noise to an $r(t)$ whose $A<|f_a(t)|$ improves the quality of the $f(t)$ that can be reconstructed within the entire T.

The wavelet transform $W_g f(s,b)$ of $f_a(t)$ with respect to the mother wavelet $g(t)$ is given by the cross-correlation between $f_a(t)$ and the daughter wavelets $g_{sb}^*(t)$ of $g(t)$ [1]:

$$W_g f(s,b)=\frac{1}{|s|^{1/2}}\int_{-\infty}^{\infty} g^*\left[\frac{t-b}{s}\right] f_a(t)\,dt$$
$$=g_s^*(b)\otimes f_a(b)=g_s^*(-b)\circ f_a(b)\ , \qquad (1)$$

where $g_s(b)=|s|^{-1/2}g(b/s)$, and s and b are the respective scaling and shift parameters. The symbols $\otimes$ and $\circ$ denote correlation and convolution operations, respectively. If $g(t)$ is complex, i.e., $g(t)=g_R(t)+jg_I(t)$ where $g_R(t)$ and $g_I(t)$ are its real and imaginary components, and $j=\sqrt{-1}$, then

$$W_g f(s,b)=W_{gR}f(s,b)+jW_{gI}f(s,b)\ .$$

Using the convolution theorem, the Fourier transform $\Omega_s(\beta)$ of $W_g f(s,b)$ can be expressed as

$$\Omega_s(\beta)=G_s^*(-\beta)F(\beta)=|s|^{1/2}G^*(-s\beta)F(\beta)\ ,$$

where $F(f)$ and $G(f)$ are the respective Fourier transforms of $f(t)$ and $g(t)$, and β and f are frequency vari-

*Electronic address: csaloma@nip.upd.edu.ph

ables. The $G(f)$ satisfies the admissibility condition $\int |G(f)|^2 |f|^{-1} df = c_g < \infty$, which implies that $G(0)=0$. Both $g(t)$ and $G(f)$ are smooth and concentrated in their respective domains. In general $G(f)=G_R(f)+jG_I(f)$ but when $g(t)$ is real then $G_R(-f)=G_R(f)$ and $G_I(-f)=-G_I(f)$.

In practice, the b value in Eq. (1) is chosen discretely: $b=kb_0$, where k is an integer and b_0 is a fixed translation parameter. Hence,

$$\Omega_s(n)=|s|^{1/2}F(n)G^*(-sn) \tag{2}$$

where $\beta=n/T$. The integer n is bounded according to $|n| \le T/b_0$. The WT analysis of $f(t)$ is done at various sizes of b_0 and at different s values. With respect to the information content in $\{t_i\}$, the smallest meaningful size for b_0 is Δ.

We now show an efficient way of computing $\Omega_s(n)$ directly from $\{t_i\}$. Because $G(f)$ is known *a priori*, Eq. (2) can be immediately evaluated once $F(f)$ is known. The $W_g f(s,b)$ is obtained by inverse Fourier transforming $\Omega_s(n)$ for all possible s values. A $2M$th-degree polynomial representation of $f(t)$ can be formulated from its Fourier series expansion:

$$\begin{aligned} f(t)&=\sum_{m=-M}^{m=M} F(m)\exp(j2\pi\delta t_i)=\sum_{m=-M}^{m=M} F(m)Z^m \\ &=Z^{-M}[F(-M)+F(-M+1)Z+\cdots+F(M)Z^{2M}] \\ &=Z^{-M}\prod_{i=1}^{2M}(Z-Z_i)=Z^{-M}f(Z) \\ &=Z^{-M}[a(0)+a(1)Z+a(2)Z^2+\cdots a(2M)Z^{2M}] , \end{aligned} \tag{3}$$

where $Z=\exp(j2\pi\delta t)$, $\delta=1/2M\Delta=1/T$, $F(m)$ is the mth Fourier coefficient of $f(t)$, and $Z_i=\exp(j2\pi\delta t_i)$. To within Z^{-M}, $f(t)$ can be represented as a $2M$th-degree polynomial $f(Z)$ in Z. Because it is a polynomial, $f(Z)$ can also be expressed as a product series of its $2M$ roots $\{Z_i\}$. Carrying out the product series involving terms in $(Z-Z_i)$ yields the polynomial coefficients $\{a(i)\}$ necessary to describe $f(Z)$. To within a multiplicative constant, the $f(t)$ spectrum $\{F(m)\}$ can be determined from $\{a(M+m)\}$ using $F(m)=a(M+m)$.

Because W increases proportionately with M, a large M is necessary if $f(t)$ is to closely resemble $f_a(t)$. However, the detection and processing of a large number of SC's have to address the issues of finite circuit response and efficiency in computing $\{a(M+m)\}$ from $\{t_i\}$. Computational accuracy depends on the accuracy with which the various SC's are located within their respective Δ's [11]. A SC location is established by counting the number of clock pulses that has elapsed when the comparator output changes state [6]. Because a pulse width cannot be less than the response time δ_c of the counter, the number of pulses within T never exceeds $T/\delta_c=2M\Delta/\delta_c$. For a fixed T, a trade-off exists between M and detection accuracy because increasing M (by decreasing Δ) results in decreasing the number of clock cycles Δ/δ_c per Δ.

The reliability of the computed $a(M+m)$'s and the time needed to compute them also depend on the number of operations needed to compute them. With a $2M!$-class algorithm, spurious $a(M+m)$ values are already obtained when M exceeds 20 [9]. The erroneous results are due to rounding-off errors which are inherent in floating-point operations where numbers are represented only to within a finite value of range and precision. If the $a(M+m)$'s are computed recursively, the effect of rounding-off errors extends rapidly throughout the entire $a(M+m)$ sequence. The following M^2-class algorithm is the most efficient so far [7,9,12]:

$$a(i)=-\frac{1}{n}\sum_{q=1}^{q=i} b(q)a(i-q) , \tag{4}$$

where $b(q)=(Z_1)^q+(Z_2)^q+\cdots+(Z_{2M})^q$ and $a(0)=1$. The $a(M+m)$'s are computed recursively starting from $a(1)$. Generally, $a(M+m)$ is complex because

$$Z_i=\cos(2\pi\delta t_i)+j\sin(2\pi\delta t_i) .$$

Imposing $a(0)=1$ presets the $F(-M)$ value at unity because $a(M+m)=F(m)$. The computed set $\{a(M+m)\}$ contains not only the spectrum of $f(t)$ but also that of the reference sinusoid $r(t)$. The $r(t)$ spectrum is given by $F(-M)=a(0)=F(M+1)=a(2M)=1$. In the computation of $\{\Omega_s(n)\}$ from $\{a(M+m)\}$, only $a(1)$, $a(2)$, . . . , and $\{a(M-1)\}$ contain nonambiguous infor-

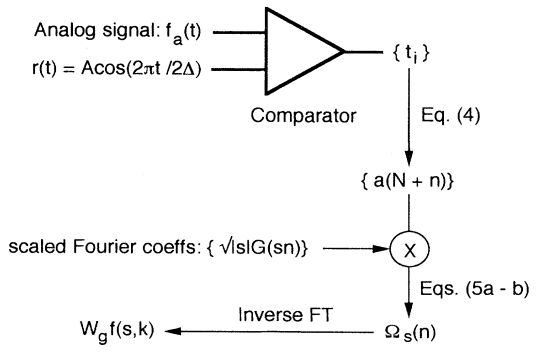

FIG. 1. Flow chart describing the computation of $W_g f(s,b)$ from the SC locations $\{t_i\}$ of $f_a(t)$.

mation about $f_a(t)$.

In general, $\Omega_s(n)=\Omega_{sR}(n)+j\Omega_{sI}(n)$:

$$\Omega_{sR}(n)=|s|^{1/2}[G_R(-sn)a_R(M+n)+G_I(-sn)a_I(M+n)]\,, \tag{5a}$$

$$\Omega_{sI}(n)=|s|^{1/2}[G_R(-sn)a_I(M+n)-G_I(-sn)a_R(M+n)]\,, \tag{5b}$$

where $a_R(M+n)$ and $a_I(M+n)$ are the real and imaginary components of $a(M+n)$, respectively. If $g(t)=g_R(t)$ then $\Omega_{sR}(n)=\Omega_{sR}(-n)$ and $\Omega_{sI}(-n)=-\Omega_{sI}(n)$ which implies that $W_gf(s,b)$ is real. In evaluating Eqs. (5), we use $a(0)=0=a(M)$. Figure 1 shows a flow chart of the procedure for computing $W_gf(s,k)$ from the $2M$ crossings of $f_a(t)$.

As a demonstration, we compute the $a(M+m)$'s pertinent to the doublet interferogram [13]

$$f_a(t)=\exp[(-x^2\sqrt{20}]\cos[2\pi 15(t-0.5)]\times\cos[2\pi 2.5(t-0.5)]\,,$$

for $0\le t\le 1$. The $f_a(t)$ is symmetric and maximum at $t=0.5$ [see Fig. 2(a)]. Analytically [13], the modulus spectrum of $|F(f)|$ of $f_a(t)$ has peaks at $f=\pm 17.5$ and ± 12.5. We use $\phi=0$, so that the length of each Δ coincides with the distance between two successive extrema of $r(t)$. Each Δ is divided into 2^q parts (clock pulses) where q is an integer. The ith SC is located within the ith interval Δ_i by finding the corresponding pulse number q_i where $[f_a(t)-r(t)]\approx 0$. The SC location t_i is given by $t_i=2^q(i-1)+q_i$, where $1\le q_i\le 2^q$.

Shown in Figs. 2(b) and 2(c) are the real and imaginary components of the $\{a(M+m)\}$ that were computed from 256 crossings of $f_a(t)$ using $\Delta=1/256$, $A=1.33f_a(0.5)$, $Z^{-M}=1$, and $q=8$. The $\{a(128+m)\}$ is complex with $a_R(M+m)=a_R(-M-m)$ and $-a_I(M+m)=a(-M-m)$ because $f_a(t)$ is real and shifted away from $t=0$. In Fig. 2(d) is the modulus $I(128+m)I=\{a_R^2(M+n)+a_I^2(M+n)\}^{1/2}$ which illustrates the doublet nature of the $f_a(t)$ spectrum.

We evaluate the effect of detection accuracy using the normalized mean square error (NMSE): $\text{NMSE}=\{\sum|f_a(k)-f(k)|^2\}/\{\sum|f(k)|^2\}$, where the summation is taken from $k=0$ to 127. The $\{f_a(k)\}$ represents 256 equally sampled values of $f_a(t)$, and

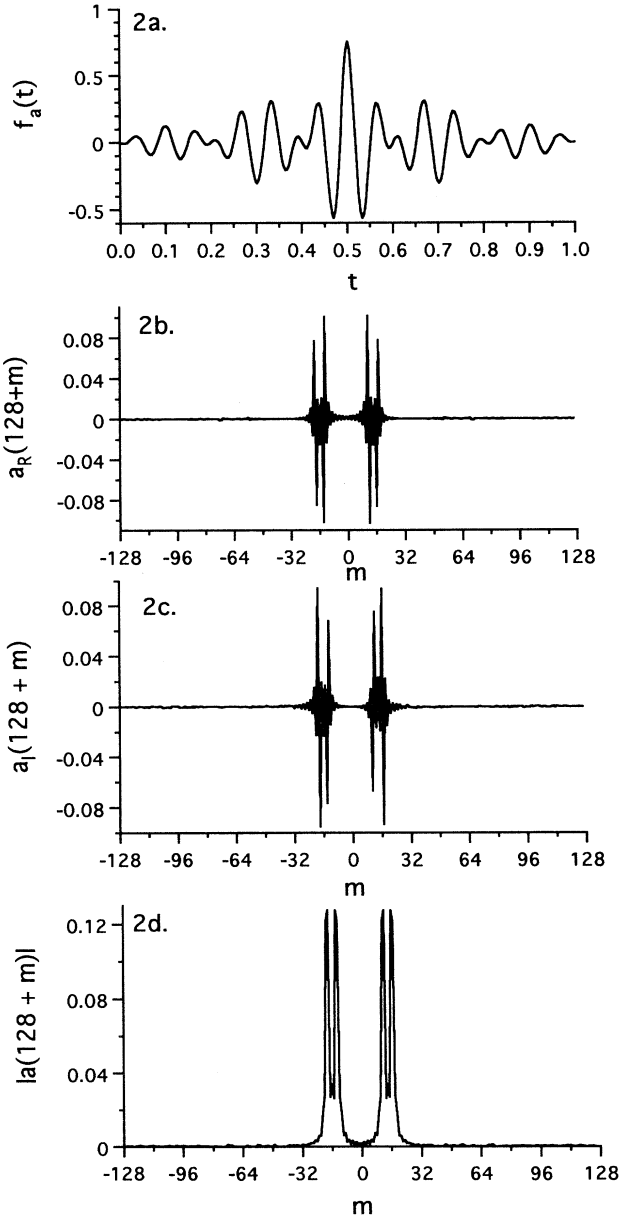

FIG. 2. (a) Test signal $f_a(t)=\exp[(-x^2\sqrt{20})]\cos[2\pi 15(t-0.5)]\cos[2\pi 2.5(t-0.5)]$, (b) $a_R(128+m)$, (c) $a_I(128+m)$, and (d) $|a(128+m)|=\{a_R^2(128+m)+a_I^2(128+m)\}^{1/2}$. The $a(128+m)$ values were computed from 256 SC's using $\Delta=1/256$ and $Z^{-M}=1$. Each D is divided into 2^8 equal parts.

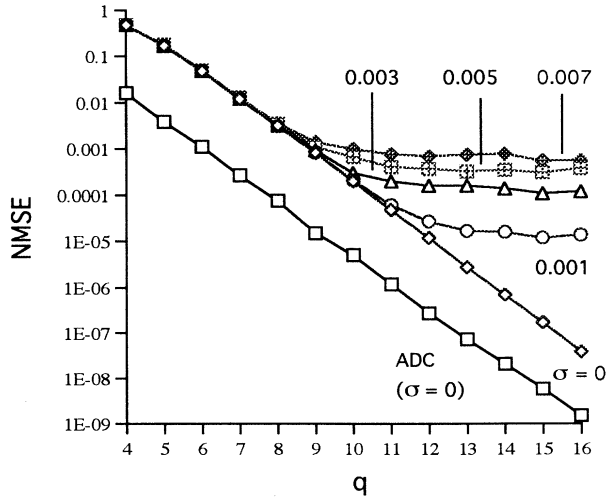

FIG. 3. Plots of NMSE vs q. In SC sampling, Δ is divided into 2^q clock cycles. The NMSE values are evaluated for increasing additive noise strengths (increasing σ). Also shown for comparison is the NMSE vs q curve ($\sigma=0$) associated with amplitude sampling by a q-bit ADC.

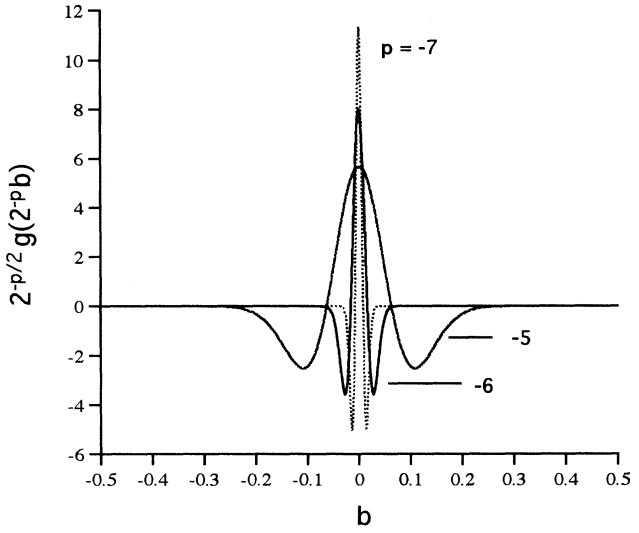

FIG. 4. (a) Plots of some sombrero-shaped wavelet basis functions $g_p(t)=2^{p/2}g(2^{-p}t)$ where $g(t)=(1-|t|^2)\exp(-|t|^2/2)$.

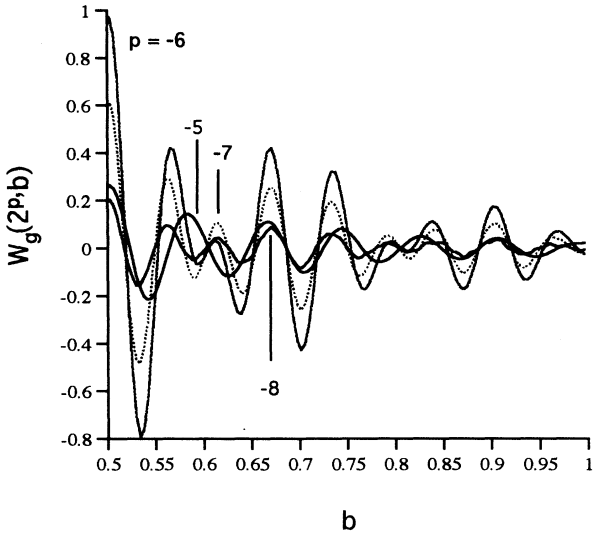

FIG. 5. Wavelet transform $W_gf(2^p,k)$ calculated using the procedure outlined in Fig. 1. It is computed from 256 sinusoidal crossings of $f_a(t)$ where $T=1$ and $b_0=\Delta=1/256$. The $W_gf(2^p,k)$ distributions are all symmetric about $t=0.5$.

$\{f(k)\}$ is the signal obtained by inverse Fourier transforming the 256 computed $a(128+m)$ values with $a(0)=0$. Shown in Fig. 3 is the NMSE vs q curve. For comparison we show also the NMSE vs q curve associated with the amplitude sampling of $f_a(t)$, by a q-bit analog-to-digital converter (ADC) whose compliance range is $2A$. Note that a q-bit ADC samples at a finite amplitude resolution of $2.66f_a(0.5)/[2^q-1]$. Note that SC detection at an accuracy of 1 in 2^{11} yields a reconstructed $f(t)$ similar to that produced by an eight-bit ADC.

We also studied the performance of SC-based sampling in the case of a noisy signal $[f_a(t)+n(t)]$ where $n(t)$ is the Gaussian noise term [14]

$$n(t)=(2\sigma^2\ln[1/\{1-A(t)\}]\cos\theta(t))^{1/2},$$

$\theta(t)=2\pi B(t)$, σ^2 is the noise variance, and $A(t)$ and $B(t)$ are randomly generated numbers in the range [0,1]. Shown in Fig. 3 is the NMSE vs q curve for $\sigma=0.001$, 0.003, 0.005, and 0.007. The NMSE deteriorates with σ. Even for noisy signals, an eight-bit ADC is still equivalent to SC detection at an accuracy of 1 in 2^{11}. Signal acquisition of noisy signals has already been demonstrated using an actual SC detector [6].

We compute the $W_gf(s,b)$ with respect to the sombrero-shaped mother wavelet [15]

$$g(t)=(1-|t|^2)\exp(-|t|^2/2)=g^*(t).$$

The Fourier spectrum $G(f)$ of $g(t)$ is real and even:

$$G(f)=G_R(f)=4\pi^2f^2\exp[-2\pi^2f^2]=G_R(-f).$$

Shown in Fig. 4 are plots of $g_s(t)$ for $s=2^{-5}$, 2^{-6}, and 2^{-7}, and in Fig. 5 are relevant $W_gf(2^p,b)$'s that were computed by inverse Fourier transforming the pertinent $\{\Omega_s(n)\}$. The $\{\Omega_s(n)\}$ were computed using Eq. (5), from the $a(128+m)$ values with $a(0)=0$ and $b_0=\Delta=1/256$ [see Figs. 2(b) and 2(c)]. A comparison of the characteristics of $f_a(t)$ [see Fig. 2(a)] and the various $g^*_{sb}(t)$'s (the relevant ones illustrated in Fig. 3) indicates that the $W_gf(2^p,b)$ shown in Fig. 5, provide a correct localized multiresolution analysis of $f_a(t)$ in terms of the sombrero-shaped wavelets. Maximum correlation between the interferogram and $g^*_{sb}(t)$ is obtained at $s=2^{-6}$ at position $b=0.5$.

In this paper, we utilized the correlation structure of $W_gf(s,b)$ together with the linearity property of Fourier transforms to show that the WT's of $f_a(t)$ can be computed directly and efficiently from its SC's with the reference sinusoid $r(t)$. To minimize the effects of rounding-off errors when M is large, an efficient algorithm for computing the coefficients $\{a(M+m)\}$ from $\{t_i\}$, was also proposed and demonstrated.

A part of this work was done with financial support from the Science and Technology Agency of Japan. The computations were done with the assistance of V. Daria and C. Blanca.

[1] S. Mallat, IEEE Trans. Pattern Anal. Machine Intell. **11**, 674 (1989); I. Daubechies, *Ten Lectures on Wavelets* (SIAM, Philadelphia, 1992).
[2] For example, see various papers: IEEE Trans. Inf. Theory, **38** (2) (1992), special issue on wavelet transforms and multiresolution signal analysis, edited by I. Daubechies, S. Mallat, and A. Willsky.
[3] See, for example, Opt. Eng. **31** (9), 1823 (1992), special issue on wavelet transforms, edited by H. Szu and H. J. Canfield; Y. Sheng, D. Roberge, H. Szu, and T. Lu, Opt. Lett. **18**, 299 (1993); L. Onural, *ibid.* **18**, 846 (1993); special issue on limited-extent waves, Appl. Opt. **33**, 5262 (1994), edited by Y. Li and Y. Zeevi.
[4] See, for example, R. Martinet, J. Morlet, and A. Grossman, Int. J. Pattern Recognition Artif. Intell. **1**, 273 (1987); H. Wit and P. van Dijk, Hear. Res. (Netherlands) **73**, 141 (1994); D. Newland, Nature **370**, 21 (1994).
[5] See, for example, E. Freysz *et al.*, Phys. Rev. Lett. **64**, 7745 (1990); M. Farge, Annu. Rev. Fluid Mech. **24**, 395 (1992); L. Hudgins, C. Friehe, and M. Mayer, Phys. Rev. Lett. **71**, 3279 (1993); K. Cho, T. Arias, and J. Joannopoulos, *ibid.* **71**, 1808 (1993); W. Langer, R. Wilson, and C. Anderson, Astrophys. J. Lett. **408**, 1 (1993); T. Thakor *et al.*, IEEE Trans. Biomed. Eng. **40**, 1085 (1993); J. Norris *et al.*, Astrophys. J. **424**, 540 (1994); B. Turner *et al.*, J. Geophys. Res. **99**, 1919 (1994); M. Holschneider, Commun. Math. Phys. **160**, 457 (1994).
[6] C. Saloma and V. R. Daria, Opt. Lett. **18**, 1468 (1993).
[7] C. Saloma and P. Haeberli, Opt. Lett. **16**, 1535 (1991).
[8] C. Saloma and M. Escobido, Jr., Appl. Opt. **33**, 7617 (1994).
[9] C. Saloma, Opt. Lett. **20**,1 (1995).
[10] C. Saloma, J. Appl. Phys. **74**, 5314 (1993).
[11] K. Weisenfeld and F. Moss, Nature **373**, 33 (1995).
[12] A. Montowski and M. Stark, *Introduction to Higher Algebra* (Pergamon, Oxford, 1964), p. 360.
[13] R. J. Bell, *Introductory Fourier Transform Spectroscopy* (Academic, New York, 1972), p. 47.
[14] J. Proakis and D. Manolakis, *Introduction to Digital Signal Processing* (Macmillan, New York, 1989), p. 132.
[15] D. Marr and E. Hildreth, Proc. R. Soc. London Ser. B **207**, 187 (1980).